AJCHE 2012, Vol. 12, No. 1, 1 – 10

Characteristics of Flame Shapes and Map For LPG and Hydrogen Inverse Confined Diffusion Flames at High Level of Fuel Excess

***Yazid Bindar*[*,1]**
***Anton Irawan*[2]**
[1]*Research Group on Energy and Processing System of Chemical Engineering, Chemical Engineering Program Study, Faculty of Industrial Technology, Institut Teknologi Bandung, Bandung, Indonesia*
[2]*Departement of Chemical Engineering, Faculty of Engineering,Universitas Sultan Ageng Tirtayasa , Serang, Indonesia*
[*]*e-mail:* yazid@fti.itb.ac.id

A combustion flame can be generated by locating the air jet supply inside the fuel jet supply. This flame is referred as an inverse diffusion flame. The size and structure of inverse diffusion flame were studied experimentally. The experiment was conducted for LPG and Hydrogen fuels. The inlet fuel and air flow rates are supplied at high level of fuel excess for its combustion reaction. These two fuels generated the flame shape having two parts. At lower part, the flame is wider and serves as a base of the flame. The upper part is longer and acts as a flame tower. The base flame was a weak flame resulted by a rich fuel-air mixture. The tower flame is formed by mixing between the entrained fuel and the air. The flame length decreases with the increase on the momentum ration between fuel and air. The flame height correlates to the fuel and air Reynold number ratio, Re_{fu}/Re_a. The development of the flame shapes from continues to strong base-tower flame shape is mapped by air and fuel inlet momentum rate. Very low fuel and air momentum rates result laminar flame and continuous shapes. The turbulent flames having base-tower shape are formed at high air momentum rate. The oxygen profiles shows that the oxygen concentration decays from the burner tip, vanishes at some distance from the burner tip and increase again after this distance. The hydrogen is completely consumed before the flame tip is reached

Keyword: Flame, Inverse, Diffusion, Laminar, Structures, Shape

INTRODUCTION

The flames from burners for the diffusion flame type are generated by supplying the fuel and the air to form combustible mixture. When the fuel supply out of the burner tip is surrounded by the air supply, the flame is called as a normal diffusion

flame. In different case, the air supply is inversely located from the normal diffusion flame case. The latest flame is categorized as an inverse diffusion flame.

One may not be familiar to the application of the inverse diffusion flame. The combustion air is injected at the central of the secondary reformer in the Ammonia plant. The gas fuel that is dominantly composed by Hydrogen (H_2) surrounds the combustion air. The generated flame is an inverse flame diffusion. Moreover, the air is supplied in amount of much below the stoichiometric portion. In this case, the amount of supplied fuel is much above the amount of the stoichiometric fuel. In other application, the pure oxygen is injected through an oxygen burner to the synthesis gas that contents more than 70 % H_2 in an transfer-line pipe . The oxygen is supplied only to combust a very small portion of the incoming H_2. The resulted flame is an inverse flame diffusion at high excess of fuel.

The inverse diffusion flame get less attention to be applied in industrial burners than the normal one. A cluster of inverse diffusion flame was applied for an industrial burner by Fleck (1998). Their test results were reported to emit very low NO_x emission (below 20 ppm at 3% O_2 for natural gas fuel). The phenomena link to the existence of strong-jet/weak-jet problem(Grandmaison at al. 1998).

Structure of NO_x concentration and temperature in an inverse diffusion flame was studied experimentally by Partridge at al. (1999) for ethane fuel. At near field region, peak zones for both NO_x and temperature locate at r/R=1/3 to 2/3. The NO_x concentration corresponds to the temperature. Further to downstream, the structures arrive on fully developed behavior.

Other interests in the study of inverse diffusion flame were soot and carbon monoxide structures. The soot from this type of flame was found to be stickier and more viscous, Arthur et al. (1958). Similar studies on the soot formation were reported by authors of Makel and Kennedy (1994) and Kang et al. (1997). Carbon monoxide was formed in the fuel side and diffuses away from the reaction zone radially into the surrounding fuel stream, Sidebotham and Glassman (1992).

It is well known that the inverse diffusion flame has a stability problem. This is one of the reasons for the applicability of the inverse diffusion flame. The map of the flame stability was investigated by Wu and Essenhigh (1985) for the methane fuel. The flame types span from unstable flame, buoyancy-sensitive blue flame, stable flames, weak and strong blue flames.

A classical flame length development for a normal diffusion flame is described as the increase of the flame length with the fuel flow rate from laminar to turbulent regimes. The flame length correlation for a normal flame length has been developed comprehensively by many authors, one of them by Becker and Liang (1978). It is different for inversed diffusion flames. The flame length regimes and correlation have not been studied so much. The reason might be on its rare application. The two characteristics of the inverse flame diffusion flame are determined by the fuel and air source momentums from jets.

An injection of pure oxygen or air into the environment hot gases (mixture of hydrogen and carbon monoxide gases) is

commonly found in metal and chemical unit processes. Its purpose is mainly to increase the hot gas temperature to meet the process demand. Part of the gas is consumed by the combustion reaction with supplied oxygen or air. This combustion acts as an inverse diffusion flame in which the oxygen or air supply surrounds by the fuel supply.

For a specific case, the pure oxygen must be distributed at the centerline of large diameter pipe in where the hot process gases (mainly hydrogen) flow inside. This case deals with an inverse diffusion flame. The flame is in the condition of high level of fuel excess. The problems to be concerned here are that what is the flame length, how the flame structure near the oxygen distributor (burner), how to create the flame zone away from the oxygen distributor tips, how far from the burner tip the oxygen concentration completely disappears.

To fill the information gap for inverse flame characterizing parameters as described above, the present work is set to serve several specific objectives. Those objectives are to describe the inverse flame length regimes, the flame shapes, flame length correlation, and global flame structures. The flame inputs are characterized by high level of fuel excess in term of the supplied fuel mixture fraction f_{sp} to be richer than its value at upper flammability limit.

FUNDAMENTAL

When fuel and oxidant are supplied separately to the mixing volume, the combustion reactions occur to generate high temperature combustion gases within that volume. The gas volume forms visually the luminous or non-luminous flame. This combustion phenomenon is classfied as a diffusion flame or non-premixed flame. The rate of combustion is determined by the the rate of mixing at the molecular level between fuel and oxidant.

The configurations of supplied fuel and the oxidant in the diffusion flame can be arranged as the fuel suply surrounded by the oxidant, Fig. 1.a, and the oxidant surrounded by the fuel, Fig. 1.b. The first one is reffered as a common diffusion flame or just diffusion flame and the second is called as an inversed diffusion flame (IDF).

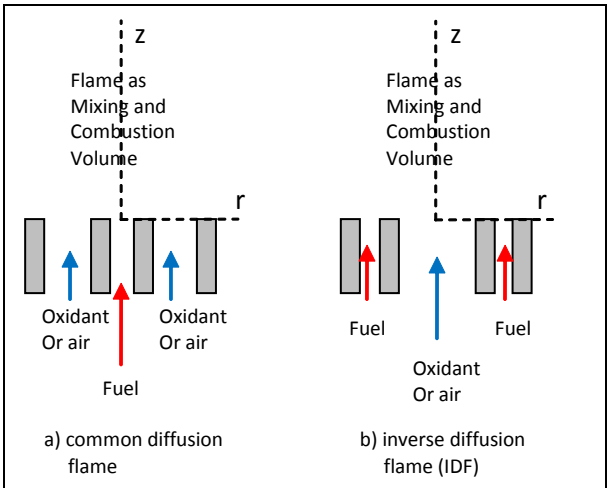

Fig. 1: Configurations of common and inverse diffusion flames

The flame structure behaviours for an ordinary diffusion flame are well established theoritically, experimentally and numerically. The flame structures characterize the profiles of involved mass fraction of chemical species i, Y_i, temperature T and the flame shape. Thelaminar flame structures are constructed in a cylindrical volume with z-axial and r-radial dimensionsunder axis-symmetric condition from the governing equations of Y_i and T as follows

$$\rho\frac{\partial Y_i}{\partial t}+\frac{1}{r}\frac{\partial(\rho v_r Y_i)}{\partial r}+\frac{\partial(\rho v_z Y_i)}{\partial z}=\frac{1}{r}\frac{\partial}{\partial r}\left(\rho r D_i\frac{\partial Y_i}{\partial r}\right)-\dot{w}_i \quad (1)$$

$$\rho\frac{\partial(c_pT)}{\partial t}+\frac{1}{r}\frac{\partial(\rho v_r c_pT)}{\partial r}+\frac{\partial(\rho v_z c_pT)}{\partial z}=\frac{1}{r}\frac{\partial}{\partial r}\left(\rho r k\frac{\partial(c_pT)}{\partial r}\right)-\Delta H_c\dot{w}_F \quad (2)$$

The axial v_z and radial v_r velocity components are obtained from the momentum governing equations. The rate of reaction for chemical species i is stated as $\dot{w}_i$. For the fuel chemical species, i=F, the rate of reaction is $\dot{w}_F$ and the combustion reaction enthalpy is ΔH_c.

Considering the fuel composed only the hydrocarbon C_xH_y and the oxidant by Oxygen O_2 and Nitrogen N_2, a fuel mixture fraction f in a finite volume of the combustion zone, is defined as the ratio between the mass of fuel origins (mass of Carbon,m_C, and mass of Hydrogen, m_H, elements), and the total mass of fuel and oxidant origins (mass of C, H, O, and N elements) as is stated in Eq. (3)

$$f=\frac{mass\ \text{of fuel origin}}{\text{mass of fuel origin}+\text{mass of oxidant origin}}=\frac{m_C+m_H}{m_C+m_H+m_O+m_N} \quad (3)$$

Since no gain and loss in mass of elements, the mixture fraction f above is conserved and follows the rule of mixing only in which the rate of reaction for f is zero. The conservation equation for laminar mixing of mixture fraction f is stated as

$$\rho\frac{\partial f}{\partial t}+\frac{1}{r}\frac{\partial(\rho v_r f)}{\partial r}+\frac{\partial(\rho v_z f)}{\partial z}=\frac{1}{r}\frac{\partial}{\partial r}\left(\rho r D\frac{\partial f}{\partial r}\right) \quad (4)$$

A complete combustion reaction follows the stochiometric reaction between fuel F and oxidant O in which 1 kg F requires $\boldsymbol{\phi}$ kg O, the mixture fraction at stoichiometric condition is stated as f_{st} =1/(1+$\boldsymbol{\phi}$). The solution of Eq.(4) produce the profile of mixture fraction f as a function time t, z and r dimensions. The flame shape at steady state condition is defined by the envelope surface for f=f_{st} as is defined as

$$f_{st}=f(z,r) \quad (5)$$

The flame length z = L_f is obtained from Eq. (5) for r = 0.

For a very specific case of an ordinary laminar diffusion, the analytical solution for Eqs. (1), (2) and (4) by Burke-Schumann, Kuo (2005), contructs a theoritical flame shape. When Burke-Schumann approach is applied for inverse flame diffusion, the boundary conditions will be definitely different. The solution,of course, will be different.

Since, the inverse diffusion flames got less attention, no basic theory so far on this flame is maturely developed. For that reason, the comprehensive experimental investigations on the inverse flame diffusion are very much required.

EXPERIMENTAL METHODS

The inverse flame diffusion is generated by a simple concentric-tube burner inside a vertical experimental furnace. The inner and outer tubes have 6.34 and 12.7 mm inside diameters respectively. The burner is placed axially at the furnace centerline.

The flame is confined in a box-type experimental furnace to avoid the air entrainment from atmosphere. The furnace has the outside dimension 40 cm x 40 cm x 180 cm. The side walls are isolated with

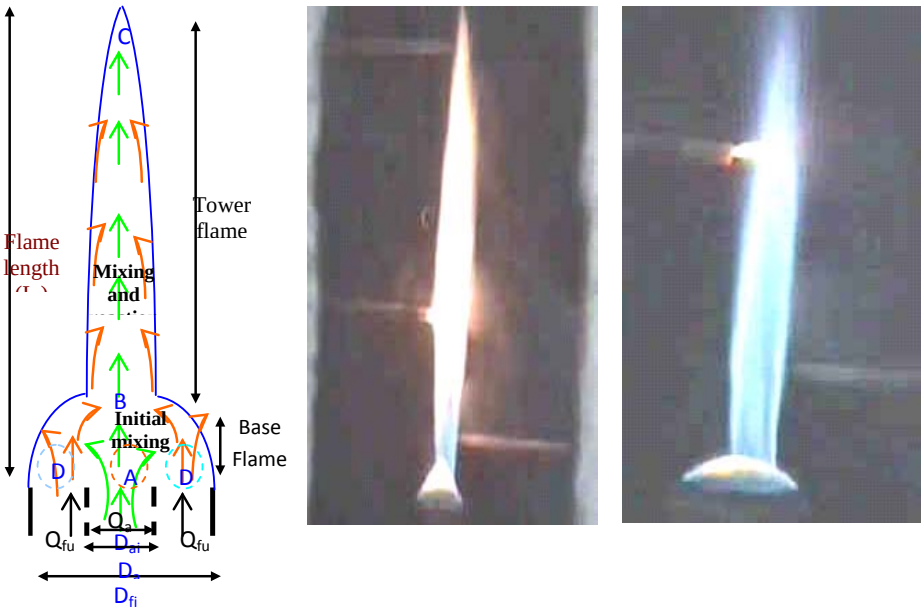

Fig. 2: Sketch and pictures of inverse diffusion flames for LPG fuel

ceramic fiber block with the thickness of 40 mm. The furnace is equipped with a long sight glass on one of the side walls to observe the flame visually. The dedicated ports are located axially for gas sampling and thermocouple tip access to the flame.

The gas temperature is measured by using Pt/10% Rh-PT thermocouples having the size 0.005 inch diameter. The gas is sampled through a sampling tube and analyzed its composition using a gas chromatography. The flame is recorded using a digital video camera. The flame length is measured directly from visual observation and recorded flames.

The preliminary experiments was conducted for the LPG fuel. The air velocity at the burner tip ranges from 3 to 9 m/s. The experimental variables are the supply fuel mixture fraction was varied from 0.146 and 0.375. These values are much higher than its stoichiometric value, that is 0.06. More comprehensive investigation was conducted for hydrogen fuel. The air velocity and the supply fuel mixture fraction vary from 2.6 to 13.2 m/s and from 0.004 and 0.05 respectively. The stochiometric fuel mixture fraction for hydrogen is 0.019. The inlet air velocity is about ten times the inlet fuel velocity.

RESULTS AND DISCUSSION

The observed flame shape of the inverse flame diffusion for LPG fuel is sketched by Figure 2. The shape is formed by two parts of flame region. The lower part is considered as a base flame. The upper part is called as a tower flame. This kind of shape is obtained at slightly higher air inlet velocity or air inlet momentum. The inlet air velocity is 5 – 16 times higher than the inlet fuel velocity. At low air flow velocity, the flame shape is similar to the normal diffusion flame shape. Higher air velocity provides the momentum for mixing process through an entrainment mechanism. The initial mixing of air and fuel occurs at the near field region, A and D regions. The fuel concentration in the A region is low, so the gas mixture would be

lean in fuel. At the D area, the fuel mixes with air both from the supplied air jet and from entrained air. The air entrainment from the ambient air envelope is weak at the jet closer to the source. The gas mixture at this D area would be rich in fuel. The flame color was red and weak at this region.

The flame length is influenced by both fuel and air momentum rates. Their effect on the flame length is explored using the relation between the ratio of flame length L_f and the inlet air pipe diameter D_s and the ratio of inlet fuel to inlet air momentum. The flame length regimes are defined by this relation as is shown in Figure3. The turbulent flame regime occurs at momentum ratio $G_{fu}/G_a < 0.025$. At this regime, the flame length does not change significantly with the momentum ratio. Increasing the momentum ratio G_{fu}/G_a from 0.025 to 0.05, the flame length increase drastically. This regime is considered as a transition regime between laminar and turbulent flame. At laminar regime, $G_{fu}/G_a > 0.055$, the flame length relation to the momentum ratio changes from steep to less steepincrease.

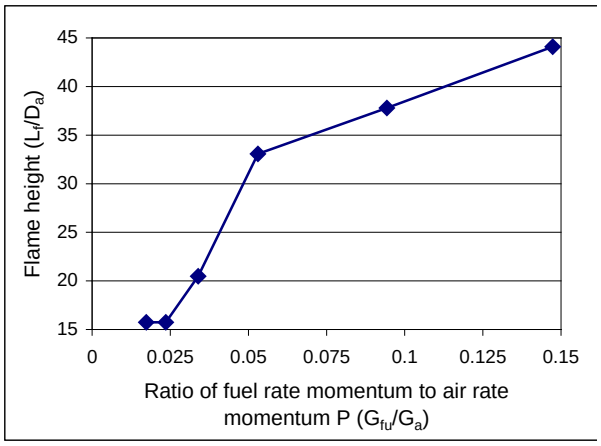

Fig. 3: Flame length regimes affected by ratio of fuel to air momentum ratio

The increase of the air velocity results intensive mixing between fuel and air at a narrow area. The high air momentum also enhance the intensity of the fuel entrainment to the air jet. The narrow area occurs due to high intensity of fuel entrainment The entrained fuel spreads to the downstream to mix with the entrained air from ambient. At this region, the tower flame is established.

The inverse diffusion flames are much less stable than normal diffusion flames. The flame combustion is stable if the balance between energy and with mass transfer can be maintained at combustion reaction zones. The ratio between the energy transfer and mass transfer is characterized by the Lewis number. If the Lewis number is larger than unity, the energy transfer rate is higher than mass transfer rate. The LPG inverse flame diffusion is less stable than the hydrogen inverse flame diffusion. This is due to higher energy transfer rate for the LPG flame than the hydrogen flame. This is indicated by the Lewis number of LPG fuel that is 1.86.

The shape development of inverse flame diffusion is explored using the hydrogen fuel. The hydrogen flames are more stable than the LPG flames. The visualization of the inverse diffusion flame shape was conducted by increasing the air flow rate $Q_a$from 5.10^{-3} – $2.5.10^{-2}$ Nm^3/minute at constant fuel flow rate Q_{fu} .In fact, at lower air momentum rate, the flame shape is no different than a normal diffusion flame shape, flame shape type I in Figure. 4. The type of inverse diffusion flamesare categorized in five shapes. The phenomena of thses flamesare explaineddescriptively inFigure 4.

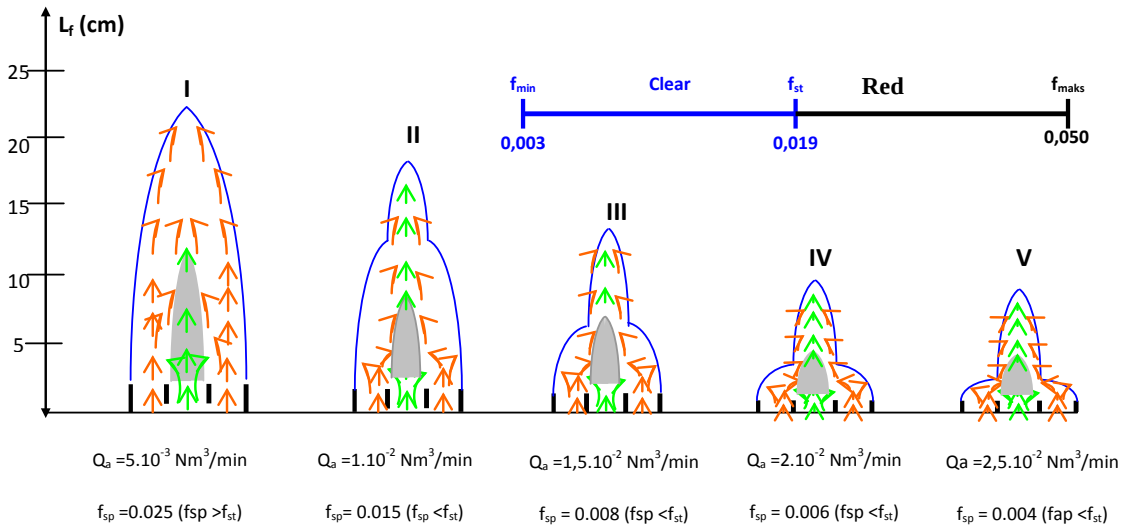

Fig. 4: Visualization of the inverse diffusion flame shape development for Hydrogen fuel

The flame starts to shrink at down stream near the flame tip when the air flow rate is increased. This is shown as theflame type II in Figure4. The total flame length is shorter than that of flame type I. Further increase of the air flow rate, the shrunk flame location shifts to upstream of the flame. The shift of this location is followed by the decrease of the flame length until reaching a constant flame length. The continuing flame development for the above condition is identified as the flame types III, IV and V as shown in Figure4.

The main variables that determine the flame types are the air and fuel momentums. The air flux momentum, G_a/A_a, is defined as the inlet momentum, $G_a=m_aU_a$, per air inlet cross section area A_a. The fuel flux is defined in a the same way that is G_{fu}/A_{fu}. The flame region is mapped byFigure 5 using these two variables. Flame type mainly occurs at high fuel flux momentum (G_{fu}/A_{fu} > 0.003) and at low air flux momentum (10 < G_a/A_a < 200). Flame type II has wider region for both fuel flux momentum (0.01 < G_{fu}/A_{fu} < 0.055) and air momentum (10 < G_a/A_a< 200). The flame type moves from type II to types III, IV and V at low fuel momentum when the air flux momentum is further increased.

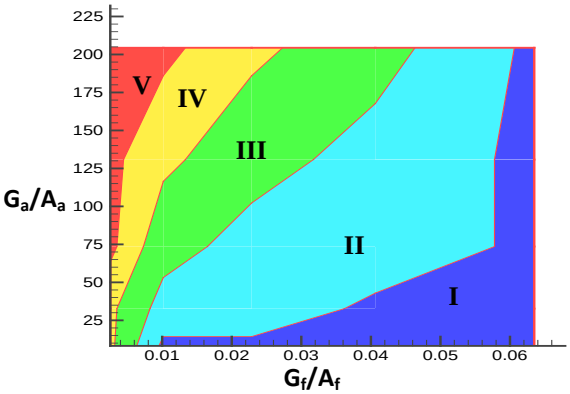

Fig. 5: The shape-map for inverse diffusion flames of Hydrogen fuel

The flame length is a function of both fuel and air momentums. The dimensionless of inlet momentum rate is defined by the Reynold number. Then, the dimensionless flame length (the ratio of the flame length and the inlet air pipe diameter, L_f/D_a) is now a function of inlet fuel Reynold number Re_{fu} and inlet air Reynold number. From the present data, the flame correlation is obtained as the following equation

$$\frac{L_f}{D_a} = 3{,}34\,\mathrm{Re}_f \left(\frac{\mathrm{Re}_f}{\mathrm{Re}_a}\right)^{0,5} \quad (6)$$

Equation (6) is expanded into the following the equation

$$\frac{L_f}{D_a} = 3{,}34 \left(\frac{D_a}{D_{fu}}\right)^{0,5} \left(\frac{\mu_a}{\mu_{fu}}\right)^{0,5} \left(\frac{1-f_{sp}}{f_{sp}}\right)^{0,5} \mathrm{Re}_f \quad (7)$$

The above correlation is well fitted to the experimental data as shown in Figure 6.

The temperature structure was obtained from the gas temperature measurement at axial and radial locations. This measurement was conducted only for hydrogen fuel. The measured temperatures are presented in contour graphs to show the flame temperature distribution, Figure 7. At high air flow rate and the same supplied fraction mixture f_{sp}, high temperatures locate near the burner tip area.

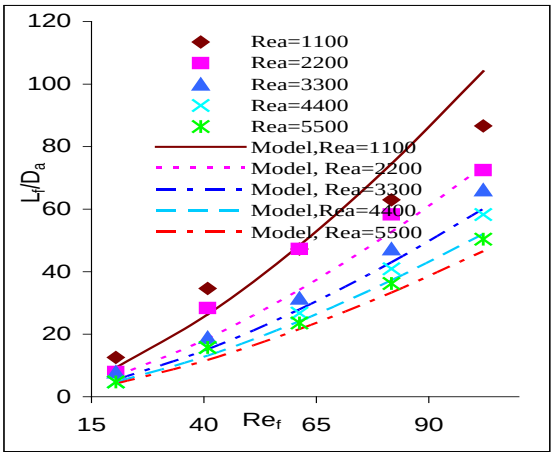

Fig. 6: Fitting the flame length correlation to the experimental data

The maximum gas temperature can be used as an indicator for the change in the temperature structure due the change of other variables is can be given by high temperature, flame tip temperature and the location of height temperature. Comparing the temperature structure for the flames at the same values of supplied fraction mixture f_{sp}, increasing the air and the fuel flow rate leads to the increase of the maximum temperature. Beside that, the location of the maximum temperature moves closer to the flame tip (Z/L_f=1), Table 1.

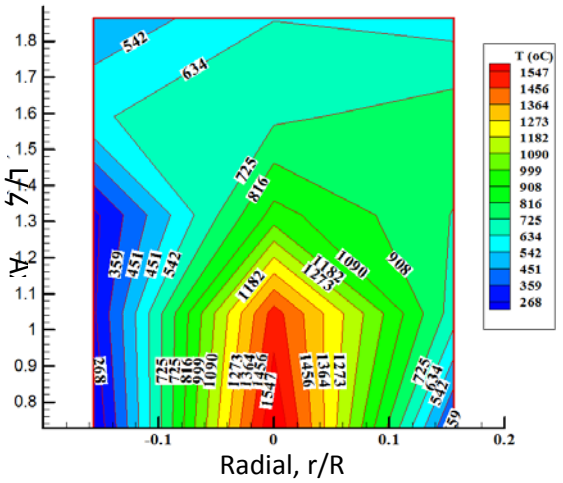

Fig. 7: Temperatur distribution in the hydrogen flame
(Q_a = 2..10^{-2}Nm^3/menit, Q_{fu} = 4.10^{-3} Nm^3/menit, f_{sp} = 0,015 or U_a=10,53 m/s, U_{fu}= 0,702 m/s)

Even though the present inverse diffusion flame was generated inside the confined box, the diffusion of the ambient air to the flame still exists. This was tested by measuring the oxygen (O_2) concentration outside the flame inside the box for longer time. The results confirm that the O_2 concentrations were not zero in those locations.

The axial profiles of oxygen concentration at the flame centerline are shown in Figure 8. This profiles confirm that the oxygen concentration decay from the burner tip, vanish at some distance from the burner tip and increase again after this distance. The starting locations where the O_2 concentration approaches zero move to upstream as the supplied fuel mixture fraction are increased.

Table 1. Maximum flame temperature at axial position at radial position r/R = 0 and f_{sp}=0,015

Condition	Q_a (Nm^3/min)	Q_{fu} (Nm^3/min)	Maximum T (°C)	Maximum Z/L_f	$T_{flametip,\ Z/Lf=1}$ (°C)
1	0.010	0.0022	1392	0,85	1150
2	0.015	0.0030	1550	0,94	1400
3	0.020	0.0040	1547	0,93	1500

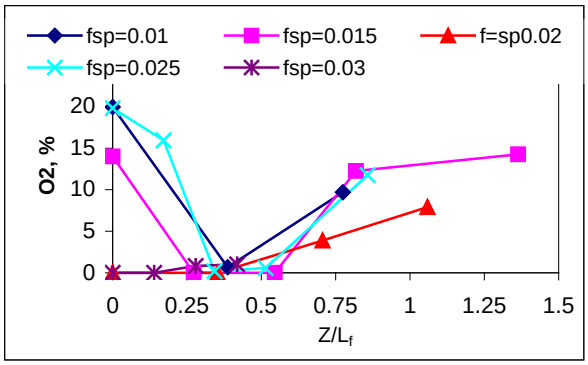

Fig. 8: Oxygen concentration profiles

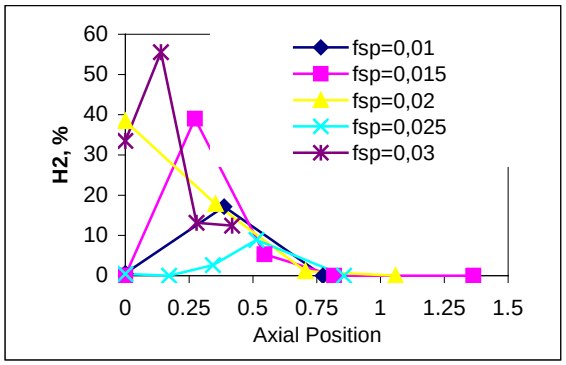

Fig. 9: Hydrogen concentration profiles

The measured hydrogen concentration along the flame center line is presented in Figure 9. The hydrogen is completely consumed before the flame tip is reached.

CONCLUSION

The shape of the inverse diffusion flame was studied for high level of excess fuel. The base and tower flame shape was observed experimentally. The base flame was considered as a weak flame resulted by a rich fuel-air mixture. The tower flame is formed by the development of mixing between the entrained fuel and the air. The flame length was decrease with increase rate momentum fuel – air ratio. The flame height is successfully correlated to the Reynold number ratio, Re_{fu}/Re_a, between the fuel (Re_{fu}) and the air jet (Re_a). The development of the flame shape from a continues flame shape to a strong base-tower flame shape is mapped by air and fuel inlet momentum rate. A very low fuel and air momentum rates result a laminar flame and continuous shape. The turbulent flames having base-tower shape are developed clearly with the increase of the air momentum rate. Turbulent flow can increase flame temperature with increase intensity of mixing fuel and air. This oxygen profiles confirm that the oxygen concentration decay from the burner tip, vanish at some distance from the burner tip and increase again after this distance. The hydrogen is completely consumed before the flame tip is reached.

ACKNOWLEDGEMENTS

The authors are grateful to Indonesian Government. through RUT VI Research Grant.

REFERENCES

Arthur, J.R., Commins, B.T., Gilbert, J.A.S., Lindsey, A.J., and Napier, D.H. (1958). Formation of polycyclic hydrocarbons in diffusion flames, Combustion and Flames, Vol. 2, pp. 267.

Becker, H.A., and Liang, D. (1978).Visible length of vertical free turbulent diffusion flames, *Combustion and Flame*, Vol.32, pp. 115.

Fleck, B.(1998). Experimental and Numerical Investigation of the Novel Low-NOx Industrial Burner, Ph.D. Thesis, Queen's University,.

Grandmaison, E.W., Yimer, I., Sobiesiak, A. and Becker, H.A., "The Strong-Jet/Weak-Jet Problem and Aerodynamic Modelling of the CGRI Burner", Combustion and Flame, 104, pp. 381,1998.

Kang, K.T., Hwang, J.Y., Chung, S.H., and Lee, W. (1997).Soot zone structure and sooting limit in diffusion flames: Comparison of counterflow and co-flow flames, Combustion and Flames, Vol. 109, pp. 266.

Kuo, K.K. (2005). Principle of Combustion, Jhon Willey & Sons, Haboboken, New Jersey, USA

Makel, D.B., and Kennedy, I.M. (1994).Soot Formation in Laminar Inverse Flame Diffusion, Combustion Science and Technology, Vol. 97, pp. 303.

Partridge, W.P., Reisel, J.R., and Laurendeau, N.M.(1999). Laser-saturated Fluoresence Measurement of Nitrix-Oxide in an Inverse Flame Diffusion, *Combustion and Flames*, Vol. 116, pp. 282.

Sidobotham, G.W., and Glasman, I. (1992).Flame Temperature, Fuel Structure, and Fuel Concentration Effects on Soot Formation in Inverse Diffusion Flames, Combustion and Flames, Vol. 90, pp. 269.

Wu, K.T., and Essenhigh, R.H., Mapping and structure of inverse diffusion flames of methane, Twentieth Symposium (International) on Combustion, The Combustion Institute, Pittsburgh, Vol. 20, No. 1, pp. 1925, 1985.